Phase diagram of ferroelectric nanowires and its mechanical force controllability

S. P. Lin, Yue Zheng' , M. Q. Cai, and Biao Wang'

Citation: Appl. Phys. Lett. **96**, 232904 (2010); doi: 10.1063/1.3446854
View online: http://dx.doi.org/10.1063/1.3446854
View Table of Contents: http://aip.scitation.org/toc/apl/96/23
Published by the American Institute of Physics

Phase diagram of ferroelectric nanowires and its mechanical force controllability

S. P. Lin,[1] Yue Zheng,[1,a)] M. Q. Cai,[2] and Biao Wang[1,a)]
[1]*State and Key Laboratory of Optoelectronic Materials and Technologies and School of Physics and Engineering, Sun Yat-sen University, Guangzhou 510275, China*
[2]*School of Physics and Miroelectronics Science, Hunan University, Changsha 410082, China*

(Received 4 February 2010; accepted 29 April 2010; published online 10 June 2010)

A phenomenological thermodynamic model of ferroelectric nanowires is developed to investigate the size-temperature phase diagrams. Considering existence of the surface tension, size, and external applied stress effects, the approximated expressions of the transition temperatures at which the paraelectric phase loses its stability with respect to the appearance of the spontaneous polarization are derived. At the same time, the size-temperature phase diagrams as functions of the ferroelectric nanowire radius are obtained, and also show its external mechanical stress controllability. © *2010 American Institute of Physics*. [doi:10.1063/1.3446854]

Nanostructures of ferroelectrics with different shape are experiencing a rapid surge of interest due to their potential usefulness in applications.[1–8] Recently, properties of ferroelectric nanostructures, including ferroelectric nanowire (FNW) and nanotube (FNT), have been theoretically and experimentally studied. Results have indicated that their properties are very sensitive to size and surface effects.[9–19]

It is well known that the "misfit strain-temperature" (MST) phase diagrams of the ferroelectric thin film (FTF) have been calculated by Pertsev *et al.*[17] using the modified Gibbs free energy. Considering size effects on phase diagrams, Morozovska *et al.*[18] gave analytical expressions for the phase diagrams of an epitaxial FTF. Based on the phase field model, Chen *et al.*[19] also developed the MST phase diagrams and domain structures of the thick FTF, Ma *et al.*[20] predicted the MST phase diagrams as function of the FTF thickness. It is noted that phase-transition characteristics of FNW should also be very much affected as functions of its size. Thus, the corresponding "size-temperature" (S-T) phase diagrams, which describe the relationship between the dimension of FNW and phase-transition temperatures, are very important in practical application involving FNWs. In this paper, we report an analytic model based on the Landau–Ginzburg–Devonshire (LGD) equation, which can be used for calculation of the S-T phase diagram as functions of the FNW sizes and external applied stress.

In the LGD equation, the spontaneous polarization $\mathbf{P}=(P_1,P_2,P_3)$ is chosen as the order parameters. The total polarization field has two components, the spontaneous polarization $\mathbf{P}$ and induced polarization $\mathbf{P}^{\mathbf{E}}$ which can be assumed to be linearly proportional to the electric field,[21–24] i.e., $\mathbf{P}^{\mathbf{E}}=\boldsymbol{\chi}_{\mathbf{b}}\mathbf{E}$, where $\boldsymbol{\chi}_{\mathbf{b}}$ are the background dielectric susceptibilities. In terms of the spontaneous polarization, the electric displacement field $\mathbf{D}$ can be written as $\mathbf{D}=\varepsilon_0\mathbf{E}+\mathbf{P}^{\mathbf{E}}+\mathbf{P}=\varepsilon_0\mathbf{E}+\boldsymbol{\chi}_{\mathbf{b}}\mathbf{E}+\mathbf{P}$. For considering enough to predict properties of ferroelectric materials under the mechanical stresses, a polynomial of expansion for bulk materials has been employed. Taking into account to the effect of the mechanical stresses, the well-known Gibbs expression function can be written as,[17]

$$\begin{aligned}\Delta G = {} & \alpha_1(P_1^2+P_2^2+P_3^2)+\alpha_{11}(P_1^4+P_2^4+P_3^4)+\alpha_{12}(P_1^2P_2^2 \\ & +P_2^2P_3^2+P_3^2P_1^2)+\alpha_{111}(P_1^6+P_2^6+P_3^6)+\alpha_{112}[P_1^2(P_2^4 \\ & +P_3^4)+P_2^2(P_1^4+P_3^4)+P_3^2(P_1^4+P_2^4)]+\alpha_{123}P_1^2P_2^2P_3^2 \\ & -Q_{11}(\sigma_1P_1^2+\sigma_2P_2^2+\sigma_3P_3^2)-Q_{12}[\sigma_1(P_2^2+P_3^2) \\ & +\sigma_2(P_1^2+P_3^2)+\sigma_3(P_1^2+P_2^2)]-\tfrac{1}{2}s_{11}(\sigma_1^2+\sigma_2^2+\sigma_3^2) \\ & -s_{12}(\sigma_1\sigma_2+\sigma_2\sigma_3+\sigma_1\sigma_3)-\tfrac{1}{2}s_{44}(\sigma_4^2+\sigma_5^2+\sigma_6^2),\end{aligned} \tag{1}$$

where α_i, α_{ij}, and α_{ijk} are the dielectric stiffness coefficients. σ_i are the stress components. s_{ij} are the elastic coefficients. Q_{ij} are the electrostrictive coefficients.

In this work, we consider a FNW with length and radius denoted by h and R, respectively, as shown in Fig. 1, which is assumed to be sandwiched between two perfect metals with the short circuit boundary conditions. Taking into account effects of the electrical and mechanical boundary conditions, the gradient and surface energies cannot be

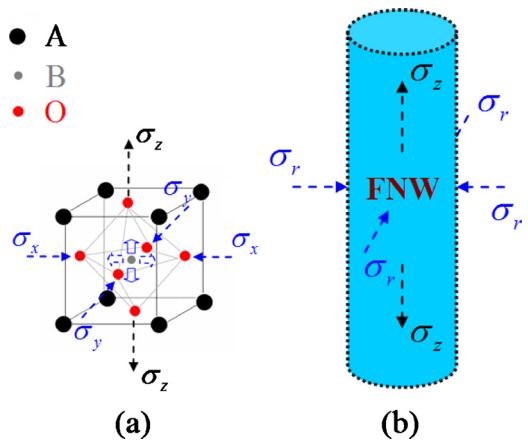

FIG. 1. (Color online) Schematic illustration of (a) the ABO_3 unit cell with compressive stresses along x and y directions and tensile stresses along z direction and (b) FNW with the surface tension effects and external applied stresses.

a)Authors to whom correspondence should be addressed. Electronic addresses: zhengy35@mail.sysu.edu.cn and wangbiao@mail.sysu.edu.cn.

neglected, which have been discussed in many literatures.[4–15] Here the gradient energy density can be written as $\Delta G_{\text{grad}}=1/2D_{ij}P_{i,j}P_{i,j}$, D_{ij} are the gradient energy coefficients.[19,20] The surface free energy G_{surf} is supposedly proportional the square of polarization on the surface.[7–13] For a FNW, the length is much larger than its radius, so we can neglect
the upper and bottom surface effects and only consider surface effect of FNW's sidewall. Then the surface energy acquires the form as $G_{\text{surf}}=2\pi R\int_{-h/2}^{h/2}[(D_{11}/\delta_1)P_1^2|_{r=R,z}+(D_{22}/\delta_2)P_2^2|_{r=R,z}+(D_{44}/\delta_3)P_3^2|_{r=R,z}]dz$, here δ_i are the so-called extrapolation length.[7,8,10,11] The depolarization field along z directions can be estimated by $E_{d3}\approx-\eta(P_3-q_e)/\varepsilon_b$, where q_e is the compensation charge density at electrodes, η can be estimated using the relation $\eta\approx1/[1+(h/2R)^2]$. In the case of a FNW, i.e., $h\gg R$, the corresponding value of η is about equal to zero, thus justifying the neglect of the depolarization field E_{d3} in the present work.[7,8] Moreover, the depolarization fields E_{d1} and E_{d2} in the x-y plane should also exist for appearance of P_1 and P_2 polarization components due to the finiteness of FNW, and can be obtained by using the electrostatic equilibrium equation $\nabla\cdot\mathbf{D}=\nabla\cdot(\varepsilon_b\mathbf{E}_d+\mathbf{P})=0$.[21–24] For FNW with the stable x-y plane polarization, the polarization components will exhibit a quasiaxisymmetric radial distribution in the x-y plane of FNW, which have been verified by molecular dynamic simulations and first principle calculations.[25,26] So we also neglect the effective influence of the x-y plane depolarization fields in following calculations.

According to recent investigations,[3,7–9] the surface layers of FNW can induce a compressive stress on the inner part. In order to study effect of this compressive stress on properties of FNW, stresses components in LGD is substituted by this compressive stresses, coefficients in LGD equation can be renormalized.[3,7–11] Based on the discussions about the renormalized coefficients of the LGD-type free energy density, we established an modified LGD equation taking into account effects of size and surface tension of FNW, and which expressions can be written as,

$$\begin{aligned}\Delta G^* = {}& \alpha_1^*(P_1^2+P_2^2)+\alpha_3^*P_3^2+\alpha_{11}(P_1^4+P_2^4+P_3^4)\\ &+\alpha_{12}(P_1^2P_2^2+P_2^2P_3^2+P_3^2P_1^2)+\alpha_{111}(P_1^6+P_2^6+P_3^6)\\ &+\alpha_{112}[P_1^2(P_2^2+P_3^2)+P_2^2(P_1^2+P_3^2)+P_3^2(P_1^2+P_2^2)]\\ &+\alpha_{123}P_1^2P_2^2P_3^2-(s_{11}+s_{12})\sigma_s^2-\tfrac{1}{2}s_{11}\sigma_z^2-2s_{12}\sigma_s\sigma_z,\end{aligned}\tag{2}$$

where α_1^* and α_3^* are dependent on the surface tension, external stress, and surface energy effects, and can be given by $\alpha_1^*=\alpha_0(T-T_{c0})+(Q_{11}+Q_{12})(\mu/R)-Q_{12}\sigma_z+(K_1/R^2)$ and $\alpha_3^*=\alpha_0(T-T_{c0})+2Q_{12}(\mu/R)-Q_{11}\sigma_z+(K_2/R^2)$,[7,11,17,27] where σ_s is the uniform compressive radial stress induce by the surface tension, given by $\sigma_s=-\mu/R$ and μ is the effective surface tension coefficient. σ_z is the external applying stress along z direction. K_1 and K_2 are coefficients determined by the gradient energy, surface effect and radius of FNW.[7,10,11]

The studies in this paper are only conducted for $BaTiO_3$ (BTO) FNW which have been fabricated and implemented recently. Since typical values of the effective surface tension coefficient vary between 5 to 50 N/m, we use a approximated value, i.e., $\mu=15$ N/m.[3,7–11,14,28] K_1 and K_2 are approximately expressed as functions of the so-called extrapolation length δ, dielectric stiffness coefficient α_0, and size-dependent parameter ζ, i.e., $K_1=\zeta_1\delta_1/\alpha_0$ and $K_2=\zeta_2\delta_2/\alpha_0$.[7] Other material constants, such as the electrostrictive and elastic coefficients are well-known.[17] According to possible phases identified by Pertsev *et al.*,[19] we only introduce the following notation for the different equilibrium phases that may occur in FNW: (i) the p phase, where $P_1=P_2=P_3=0$; (ii) the c phase, where $P_3\neq0$ and $P_1=P_2=0$; (iii) the aa phase, where $P_1=P_2\neq0$ and $P_3=0$; and (iv) the r phase, where $P_1=P_2\neq0$ and $P_3\neq0$.

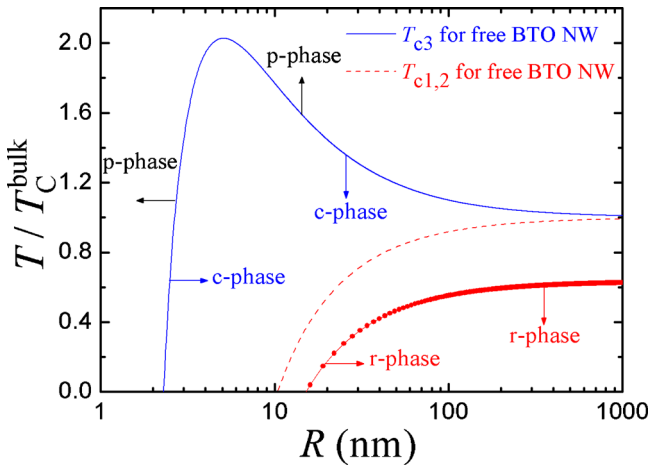

FIG. 2. (Color online) The S-T phase diagrams of free-standing BTO NW.

From the analysis of Eq. (2), it is known that the phase transition from the paraelectric state to ferroelectric states is of the first order in BTO FNWs due to the negative sign of the coefficients α_{11} and α_{12}. We only investigate the phase transitions with temperature cooling-down in following calculations. According to stability analysis,[11,17] the phase transition temperatures of $T_{c1,2}$ and T_{c3}, at which the paraelectric phase loses its stability with respect to the appearance of $P_1=P_2$ and P_3, can be obtained by setting $\alpha_1^*=0$ and $\alpha_3^*=0$. So the phase transition from the paraelectric state to ferroelectric states takes place at temperature $T_c=\max[T_{c1,2},T_{c3}]$, here $T_{c1,2}$ and T_{c3} of FNW with the external applied stress σ_z can be given by $T_{c1,2}=T_{c0}-((Q_{11}+Q_{12})/\alpha_0)(\mu/R)+(Q_{12}/\alpha_0)\sigma_z-(K_1/\alpha_0R^2)$ and $T_{c3}=T_{c0}-(2Q_{12}/\alpha_0)(\mu/R)+(Q_{11}/\alpha_0)\sigma_z-(K_2/\alpha_0R^2)$.

When we predict the boundary between r- and c-phases or r- and aa-phases, effect of nonzero P_3 on instability with respect to $P_{1,2}$ or nonzero $P_{1,2}$ on instability with respect to P_3 must be considered. The equilibrium values of the components of the polarization P_i can be determined by minimizing the free energy function of Eq. (2) with respect to the polarization. For FNW, the equilibrium phases under different radius, temperatures, and external applied stresses can be determined by minimization of the modified free energy, e.g., $\partial\Delta G^*/\partial P_i=0$.[17–20]

Firstly, we only consider the free-standing FNW, and give the S-T phase diagrams as functions of radius. In absence of the external stress load, i.e., $\sigma_z=0$, it is can be seen that $Q_{11}+Q_{12}$ are positive whereas Q_{12} is negative for BTO NWs. T_{c3} is always higher than $T_{c1,2}$, because the surface tension always enhances the phase transition temperature T_{c3}, and on the contrary decreases the phase transition temperatures $T_{c1,2}$. Results of Fig. 2 have given the normalized phase transition temperature $T_c/T_C^{\text{bulk}}=T_{c3}/T_C^{\text{bulk}}$ as function

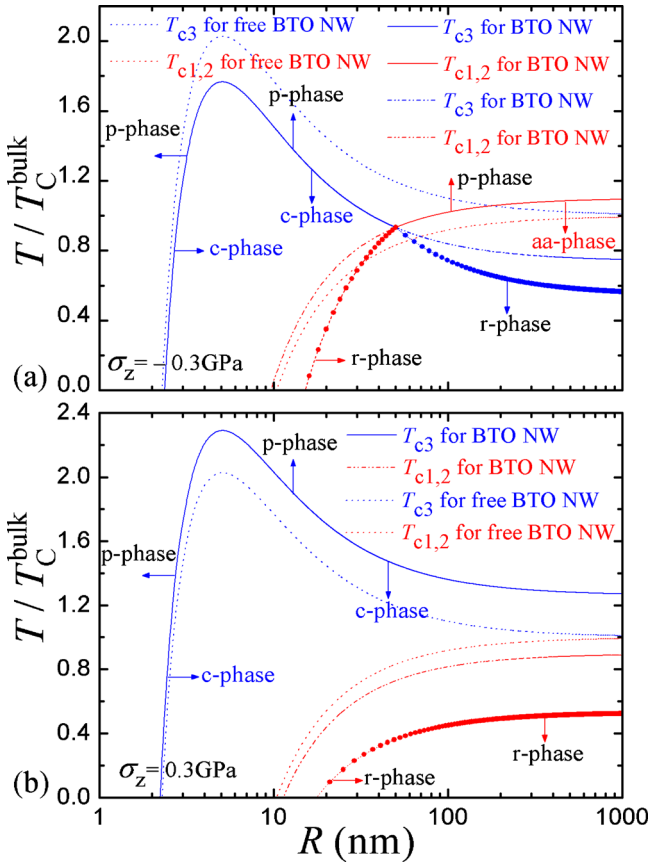

FIG. 3. (Color online) The S-T phase diagrams of BTO NW for (a) the compressive stress load σ_z=−0.3 GPa and (b) tensile stress load σ_z =0.3 GPa.

of radius R, T_C^{bulk}=383 K is the phase transition temperature from the paraelectric state to ferroelectric of BTO bulk.[17] When FNWs are in ferroelectric state, it can be seen that the *r*-phase dominates and *c*-phase shrink with the radius increasing, here red cycle line is the boundary of the *r*-phase and *c*-phase. When the radius of FNW is large, i.e., $R>100$ nm, the phase transition temperature T_c is about the value of bulk material, i.e., $T_c \approx T_C^{bulk}$. These reasons are that the compressive stress due to the surface tension decreases with the radius increasing, and is very weak for a large radius FNW.

When the external stress load is incorporated to the total free energy Eq. (2), we can develop the S-T phase diagram controlled by σ_z. It is known that the compressive stress, i.e., σ_z=−0.3 GPa, will reduce the polarization component along z direction P_3, and enhance the polarizations P_1 and P_2. Figure 3(a) shows that influence of the compressive stress on the S-T phase diagram of BTO NW. Solid blue and red line in Fig. 3(a) indicate that the phase transition T_c is T_{c3} for $R<50$ nm and $T_{c1,2}$ for $R>50$ nm, respectively, which is different with that in Fig. 2. More importantly, the compressive stress can induce appearance of the *aa*-phase, and shift the *c*-phase and *r*-phase as a whole to shrink. On the contrary, the tensile stress, i.e., σ_z=0.3 GPa, result in the *c*-phase to the high temperature as shown in Fig. 3(b). The *r*-phase obviously shrinks also due to effect of the tensile stress. In addition, we also calculated the S-T phase diagrams for BTO NW with the larger compressive and tensile stresses. Results indicate that *aa*-phase dominates with the compressive stress increasing, and *c*-phase dominates and *r*-phase shrinks with the tensile stress increasing.

In summary, we developed a thermodynamic model to investigate effects of the surface tension and external mechanical load on the S-T phase diagrams of FNWs. Calculations show that the phase transition temperatures of FNW are determined by its radius due to the surface tension and size effects. More importantly, the S-T phase diagrams can be controlled by the applied stresses. However, we should note that these approximated results need more rigorous treatment by the phase field, effective Hamiltonian or molecular dynamic simulations, and experimental confirmations.

This project was supported by grants from the NSFC (Grant Nos. 10902128, 10732100, 50802026, and 10972239) and the Open Fund of the State Key Laboratory of Optoelectronic Materials and Technologies (SYSU).

[1]M. Dawber, K. W. Rabe, and J. F. Scott, Rev. Mod. Phys. **77**, 1083 (2005).
[2]F. D. Morrison, Y. Luo, I. Szafraniak, V. Nagarajan, R. B. Wehrspohn, M. Steinhart, J. H. Wendroff, N. D. Zakharov, E. D. Mishina, K. A. Vorotilov, A. S. Sigov, S. Nakabayashi, M. Alexe, R. Ramesh, and J. F. Scott, Rev. Adv. Mater. Sci. **4**, 114 (2003).
[3]K. Uchino, E. Sadanaga, and T. Hirose, J. Am. Ceram. Soc. **72**, 1555 (1989).
[4]Y. Zheng and C. H. Woo, Nanotechnology **20**, 075401 (2009).
[5]S. S. Nonnenmann, O. D. Leaffer, E. M. Gallo, M. T. Coster, and J. E. Spanier, Nano Lett. **10**, 542 (2010).
[6]S. S. Nonnenmann, E. M. Gallo, M. T. Coster, G. R. Soja, C. L. Johnson, R. S. Joseph, and J. E. Spanier, Appl. Phys. Lett. **95**, 232903 (2009).
[7]A. N. Morozovska, E. A. Eliseev, and M. D. Glinchuk, Phys. Rev. B **73**, 214106 (2006).
[8]Y. Zheng, C. H. Woo, and B. Wang, Nano Lett. **8**, 3131 (2008).
[9]W. H. Ma, M. S. Zhang, and Z. H. Lu, Phys. Status Solidi B **166**, 811 (1998).
[10]I. I. Naumov, L. Bellaiche, and H. X. Fu, Nature (London) **432**, 37 (2004).
[11]M. Hamedoun, H. Bakrim, K. Bouslykhane, A. Hourmatallah, N. Benzakour, A. Filali, and R. Masrour, J. Phys.: Condens. Matter **20**, 125216 (2008).
[12]I. I. Naumov and H. X. Fu, Phys. Rev. Lett. **95**, 247602 (2005).
[13]Y. Zheng, C. H. Woo, and B. Wang, J. Phys. Condens. Matter **20**, 135216 (2008).
[14]M. Q. Cai, Y. Zheng, B. Wang, and G. W. Yang, Appl. Phys. Lett. **95**, 232901 (2009).
[15]Z. H. Zhou, X. S. Gao, J. Wang, K. Fujihara, S. Ramakrishna, and V. Nagarajan, Appl. Phys. Lett. **90**, 052902 (2007).
[16]W. Liu, X. H. Sun, H. W. Han, M. Y. Li, and X. Z. Zhao, Appl. Phys. Lett. **89**, 163122 (2006).
[17]N. A. Pertsev, A. G. Zembilgotov, and A. K. Tagantsev, Phys. Rev. Lett. **80**, 1988 (1998).
[18]M. D. Glinchuk, A. N. Morozovska, and E. A. Eliseev, J. Appl. Phys. **99**, 114102 (2006).
[19]Y. L. Li and L. Q. Chen, Appl. Phys. Lett. **88**, 072905 (2006).
[20]D. C. Ma, Y. Zheng, and C. H. Woo, Appl. Phys. Lett. **95**, 262901 (2009).
[21]C. H. Woo and Y. Zheng, Appl. Phys. A: Mater. Sci. Process. **91**, 59 (2008).
[22]Y. Zheng and C. H. Woo, Appl. Phys. A: Mater. Sci. Process. **97**, 617 (2009).
[23]A. K. Tagantsev, Ferroelectrics **375**, 19 (2008).
[24]M. E. Lines and A. M. Glass, *Principles and Applications of Ferroelectrics and Related Materials* (Clarendon, Oxford, 1979).
[25]Y. H. Zhang, J. Hong, B. Liu, and D. N. Fang, Nanotechnology **20**, 405703 (2009).
[26]G. Pilania, S. P. Alpay, and R. Ramprasad, Phys. Rev. B **80**, 014113 (2009).
[27]S. Lin, T. Q. Lv, C. Q. Jin, and X. H. Wang, Phys. Rev. B **74**, 134115 (2006).
[28]Y. Zheng, B. Wang, and C. H. Woo, Acta Mech. Solida Sinica **22**, 524 (2009).